CHIN. PHYS. LETT. Vol. 33, No. 2 (2016) 026102

Atomistic Simulations of the Effect of Helium on the Dissociation of Screw Dislocations in Nickel *

Jian Xu(许健)[1,2], Cheng-Bin Wang(王呈斌)[1,3], Wei Zhang(张伟)[1,3], Cui-Lan Ren(任翠兰)[1,3], Heng-Feng Gong(龚恒风)[1], Ping Huai(怀平)[1]**

[1]*Shanghai Institute of Applied Physics, Chinese Academy of Sciences, Shanghai 201800*
[2]*University of Chinese Academy of Sciences, Beijing 100049*
[3]*Key Laboratory of Interfacial Physics and Technology, Chinese Academy of Sciences, Shanghai 201800*

(Received 30 September 2015)

The interactions of He with dissociated screw dislocations in face-centered-cubic (fcc) Ni are investigated by using molecular dynamics simulations based on an embedded-atom method model. The binding and formation energies of interstitial He in and near Shockley partial cores are calculated. The results show that interstitial He atoms at tetrahedral sites in the perfect fcc lattice and atoms occupying sites one plane above or below one of the two Shockley partial cores exhibit the strongest binding energy. The attractive or repulsive nature of the interaction between interstitial He and the screw dislocation depends on the relative position of He to these strong binding sites. In addition, the effect of He on the dissociation of screw dislocations are investigated. It is found that He atoms homogeneously distributed in the glide plane can reduce the stacking fault width.

PACS: 61.72.Yx, 61.72.Bb, 61.72.Lk, 61.72.Nn, 02.70.−c DOI: 10.1088/0256-307X/33/2/026102

Ni-based alloys are potential structural materials for Gen-Ⅳ nuclear reactors, due to their good creep rupture properties and high-temperature strength.[1,2] Most structural alloy materials can produce He by (n,α) transmutation reactions in the nuclear reactor. He is insoluble in the solid matrix, and the precipitated helium atoms tend to form He-void clusters or even bubbles. The bubbles can grow easily at lattice defects, e.g., dislocations, causing degradation of macro physical and mechanical properties of the material.[3–6] Hence, He embrittlement is a crucial issue for Gen-Ⅳ reactors due to the fact that these reactors operate with a more extreme environment.[1]

Crystalline materials usually contain a large number of dislocations, which determine dramatic variations in their mechanical properties.[7,8] Experiments found that irradiation can lead to hardening of metal materials.[9] However the mechanism of the hardening was unclear. Rodney *et al.* recently suggested that the hardening is due to the defects (vacancy, interstitial clusters, etc.) produced by pinning of dislocations.[10] Xu *et al.* reported that He implantation increases the ultimate tensile strength and ductility of Ni samples with only dislocations.[11,12] A better understanding of the microscopic mechanisms of interactions between He and defects in metals is essential for the nuclear and materials industry.

Computational techniques such as molecular dynamics (MD) simulations are useful tools to study the influence of defect obstacles on the movement of the dislocation. The interaction of He-vacancy clusters with dislocations has been studied by Yang *et al.*[13] as well as interstitial He atoms with edge dislocation by Heinisch *et al.*[14] Even though previous studies have shed significant light on these issues, still some mechanisms remain unclear, and several interesting problems require further study. Moreover, the understanding of the atomic behavior of He in Ni is very limited, and especially, the details of the interactions between He and different dislocations in Ni remain poorly characterized.

In this work, the behavior of He in the presence of screw dislocation in pure Ni is investigated as well as the effect of He on the stacking fault (SF) width. The results presented here are helpful to deepen our understanding of the effects of He on the mechanical properties of metallic materials.

The molecular statics simulations in this study were performed by using the molecular dynamics code LAMMPS.[15] The interatomic potentials were originally developed by Sheng *et al.*,[16] Aziz *et al.*,[17] and Zhang *et al.*[18] to describe Ni–Ni, He–He, and Ni–He interactions, respectively. The Ni–He pair potential was fitted by using the Potfit program.[19] The potential form is

$$E_{\mathrm{Ni-He}}(r_{ij})=\begin{cases}\text{ZBL potentials,}^{[20]} & r_{ij}\le r_1,\\ P_3r_{ij}^3+P_2r_{ij}^2+P_1r_{ij}+P_0, & r_1\le r_{ij}\le r_2,\\ f_{\mathrm{fit}}(r_{ij})f_{\mathrm{c}}(r_{ij}), & r_{ij}\ge r_2,\end{cases} \tag{1}$$

where the energy conservation at the cutoff distance is realized by introducing a cut-off function $f_{\mathrm{c}}(r_{ij})$

$$f_{\mathrm{c}}(r_{ij})=A(r_{ij}-r_{\mathrm{d}})^2+B(r_{ij}-r_{\mathrm{d}})^2, \tag{2}$$

with A and B being coefficients obtained from the boundary condition at $r_{\mathrm{c}}=6.0\,\text{Å}$. The parameters are listed in Table 1.

The lattice parameter α_0 and the cohesive energy for fcc Ni are 0.35 nm and $-4.44\,\mathrm{eV/atom}$, respectively. During energy minimization, the atomic positions were relaxed through the conjugate-gradient method, with a time step of 0.5 fs and an energy tolerance of 10^{-9}. The common neighbor analysis

*Supported by the Program of International S&T Cooperation under Grant No 2014DFG60230, the Strategically Leading Program of the Chinese Academy of Sciences under Grant No XDA02040100, the Shanghai Municipal Science and Technology Commission under Grant No 13ZR1448000, and the National Natural Science Foundation of China under Grant No 11505266.
**Corresponding author. Email: huaiping@sinap.ac.cn
© 2016 Chinese Physical Society and IOP Publishing Ltd

(CNA)[21] with a cutoff of 0.30 nm was used to identify crystalline defects (i.e., non-fcc atoms),[22] and the atomic configurations were visualized by using the OVITO software package.[23]

The simulations were performed in a rectangular cell with x, y, and z axes oriented along the $[11\bar{2}]$, [111], and $[1\bar{1}0]$ directions, respectively. The dimensions of the simulation cell were $17.1\times12\times20\,\text{nm}^3$. An $\alpha_0/2[1\bar{1}0](111)$ screw dislocation was introduced into the center of the cell by using the code MD++.[24] Periodic boundary conditions (PBCs) were adopted along the z direction, while free boundary conditions were applied along x and y directions. Perfect dislocations in fcc materials are known to be unstable, dissociating easily into partial dislocations separated by stacking fault (SF) regions. The degree of dissociation is dictated by the SF energy of the material. The SF energy in Ni, determined experimentally, is $\sim125\,\text{mJ/m}^2$,[25] indicating easy dissociation of perfect dislocations. After introducing a screw dislocation into the simulation cells, an energy minimization was performed. As is expected, the dislocation is dissociated into two $\alpha_0/6\langle112\rangle$ Shockley partials separated by an SF on the [111] plane, as shown schematically in Fig. 1. The width of the SF is 1.18 nm, which agrees well with the other results (0.74–1.49 nm[26–30]).

Table 1. Parameters for the Ni–He potential.

p_3 (eV/Å^3): −882.70101	p_2 (eV/Å^2): 2725.01357	p_1 (eV/Å): −2835.46539	p_0 (eV): 1004.91061
A (eV/Å^2): −25.46824	B (eV/Å^3): −1.86999	r_d (Å): 6.05	
r_1 (Å): 0.5	r_2 (Å): 1.1		

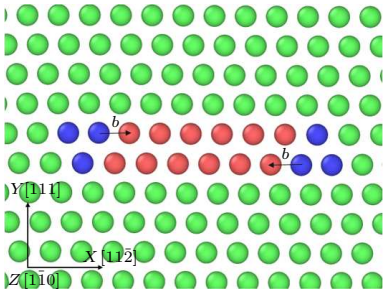

Fig. 1. Schematic diagram of the dissociated screw dislocation. The fcc Ni, Shockley partials (non-fcc atoms), and SF region (hcp atoms) are shown as green, blue, and red spheres, respectively. Here ***b*** represents the burger vectors denoted by the arrows.

Additional simulations to investigate the elastic interactions between He and screw dislocation were performed by introducing one He atom at various occupying sites in the vicinity and/or interior of the extended dislocation or giving an areal density. Energy minimization was performed after the introduction of He to obtain the equilibrium configuration. Possible interstitial sites for He occupation in the Ni are either octahedral (O sites) or tetrahedral (T sites). The stability of interstitial He atoms is judged by formation energy. In a perfect fcc Ni lattice, it is defined as

$$E^\text{f}_\text{He} = E_\text{tot}(\text{He}) - \{\varepsilon_\text{He} + E_\text{tot}\}, \tag{3}$$

where $E_\text{tot}(\text{He})$ is the total energy of the system with a single He atom, $\varepsilon_\text{He} = -0.0074\,\text{eV}$ is the calculated cohesive energy of a perfect fcc He crystal, and E_tot is the total energy of a perfect fcc Ni system, but without He. In the 'dislocated' lattice, it is defined as

$$E^\text{f}_\text{He}(\text{Disloc}) = E_\text{tot}(\text{Disloc}+\text{He}) - \{\varepsilon_\text{He} + E_\text{tot}(\text{Disloc})\}, \tag{4}$$

where $E_\text{tot}(\text{Disloc}+\text{He})$ is the total energy of the system with dislocations and one He atom, and $E_\text{tot}(\text{Disloc})$ is the total energy of the Ni system with dislocations, but without He.

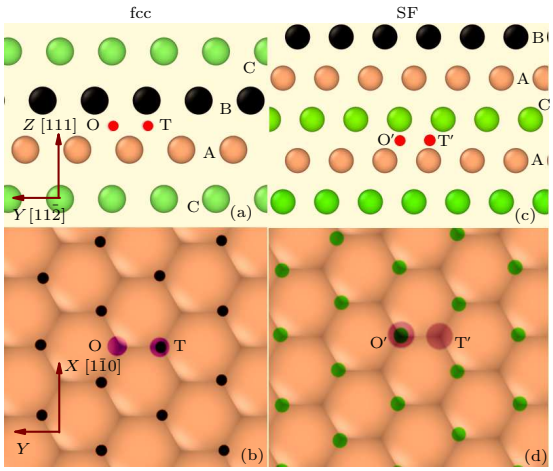

Fig. 2. (a) Side and (b) top views of the cells. Octahedral (O) and tetrahedral (T) occupying sites are indicated by small red spheres. (c) Side and (d) top views, respectively, of octahedral (O′) and tetrahedral (T′) sites, also indicated by small red spheres. Orange, black, and green spheres represent atoms on the A, B, and C planes, respectively. In (b), only A and B planes are shown; only A and C planes are shown for (d). The atoms of the A plane are enlarged for better visualizations.

In addition, the specific structure of He atoms in fcc Ni is discussed in the presence of defects. Regarding the ABCABC packing sequence of perfect fcc crystals, O sites are located on the central planes between adjacent A and B planes, overlapping with the projections of C-plane atoms, as shown schematically in Fig. 2(a). A top view of the central plane depicting only A- and B-plane atoms is also shown in Fig. 2(b). T sites in the perfect fcc lattice are also located on the central planes, while they overlap with the projection of B-plane atoms, as indicated in Figs. 2(a) and 2(b). However in SF regions, O and T sites differ from those in the perfect fcc lattice. For highly distorted lattices, the O and T sites are typically difficult to define, as the occupation sites are named based on their relations to the local lattice structure. Hence, occupation sites in the SF will henceforth be called O′ or T′ sites, with respect to the position of the site relative to the reference lattice, which is designated as the upper half

(along the z direction) of the lattice. As shown in the side view in Fig. 2(c), relative to the ACAC hexagonal close-packed (HCP) sequence of an SF, O′ sites are located just under the C-plane atoms. Meanwhile, T′ sites in the SF overlap with the projections of B-plane atoms three layers below or above, as shown in Figs. 2(c) and 2(d). As the formation energy of interstitial He at a T site (4.5 eV) was lower than at an O site (4.65 eV), T sites were found to represent the most stable sites for interstitial He in fcc Ni, in good agreement with the previous findings.[31,32] The formation energy of interstitial He at a T′ site (4.18 eV) is also lower than at an O′ site (4.55 eV). Hence, in the remaining part of this work, the interstitial He atoms are introduced in the models to occupy either T sites in the fcc structure or T′ sites in the SF region.

Additional calculations of the generalized stacking fault energy (GSFE) of the primary slip system were carried out by cutting a cell representing a perfect fcc lattice into two equal halves along a (111) slip plane, and then shearing the upper half relative to the lower half in the x direction by the fault vector f, in units of $\alpha_0/6[11\bar{2}]$. The GSFE represents the energy per unit area gained during the shearing process. The simulation cell size was $15.1 \times 15 \times 20\,\mathrm{nm}^3$. PBCs were applied along both x and z directions, and free boundary conditions were applied along the y direction. These simulations were performed for different He concentrations, introduced at T sites located between the upper and lower halves. During shearing, He atoms are able to move by a different mechanism compared with Ni atoms, due to their different atomic sizes and mobilities. During energy minimization, He atoms were forced to gradually move along a specific path, going from a T site to the neighboring O site in the shear plane as Ni atoms moved from an fcc site to an hcp site, while allowing them to relax in the z direction.

The effect of He on dislocation dissociation and generalized stacking fault energy was studied by inserting He atoms uniformly distributed in the slip plane.

The binding energies of an interstitial He to a screw dislocation were calculated as a function of its position to the dislocation centerline, which is defined as the midline between the two Shockley partials. These calculations were performed by introducing one He atom at different sites around and inside the dissociated dislocation, then minimizing the total potential energy of the system. In the central plane between the two hexagonal close-packed (hcp) sequence planes defining the dislocation glide plane, T sites were selected in areas far from the dislocations, where the crystal lattice is a perfect fcc structure, whereas T′ sites were selected in the SF region. Only T sites were selected in planes located one and two layers above and below the glide plane, since these planes have a perfect fcc lattice structure. Here the binding energies E_B of a single He atom to the dislocations are defined as

$$E_\mathrm{B}^\mathrm{s}(\mathrm{Disloc+He}) = E_\mathrm{f}^\mathrm{perfect}(\mathrm{He}) - E_\mathrm{f}^\mathrm{s}(\mathrm{Disloc+He}), \quad (5)$$

where $E_\mathrm{f}^\mathrm{perfect}(\mathrm{He}) = 4.5\,\mathrm{eV}$ is the formation energy of a He atom in the perfect Ni lattice and $E_\mathrm{f}^\mathrm{s}(\mathrm{Disloc+He})$ is the formation energy of a He atom at the S sites (i.e., T or T′ sites) in the 'dislocated' lattice.

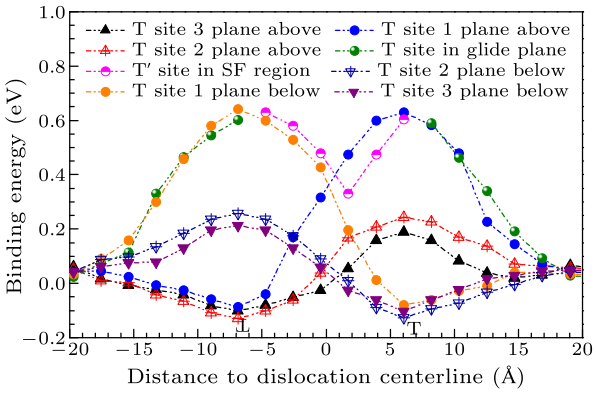

Fig. 3. Binding energies of interstitial He to screw dislocations. The positions of the Shockley partial cores are indicated by T and inverse T symbols.

The binding energies to a screw dislocation of He at different sites and on different planes are shown in Fig. 3. For He at T sites on the glide plane, the binding energy increases as the He atom approaches the dislocation centerline, and a maximum is observed at $|x| = 6$ Å. This point lies just ahead of the Shockley partial core of the screw dislocation (recall that the SF width of the screw dislocation is 11.8 Å). On the other hand, for He at T′ sites in the SF, the binding energy rapidly decreases for He atoms far from the Shockley partial cores. The minima near the dislocation centerline are obviously seen in Figs. 1 and 3. For He at T sites on planes other than the glide plane, the binding energy curves are antisymmetric with respect to the dislocation centerline ($x = 0$). This is due to the antisymmetry in the stress field that develops around the screw dislocation. A negative binding energy is obtained for He at T sites near a partial core (compression region), whereas a positive binding energy is obtained at the other cores (tension region). In planes above the glide plane, the binding energy decreases as the He atom approaches the dislocation centerline from the positive x direction, with a minimum at $x = 6$ Å. Beyond this minimum, the binding energy increases until it reaches a maximum when the He atom is at $x = 6$ Å (i.e., on the other side of the dislocation). For He on planes below the glide plane, the behavior is reversed. In this case, the binding energy decreases as He approaches the dislocation centerline from the negative x direction, with a minimum at $x = 6$ Å followed by an increase to a maximum at $x = -6$ Å. In addition, in the partial cores, the tetrahedral interstitial He atoms spontaneously assume a [110] direction 'Crowdion' configuration, as shown in Fig. 4.

It is clear that the Shockley partial cores of a screw dislocation have the strongest interactions with interstitial He atoms. The strongest attractive interaction is observed for He atoms located one plane above or below the slip plane, and the strongest repulsive interaction is observed for He atoms located two planes above or below the glide plane. Meanwhile, the attrac-

tive or repulsive nature of the interaction between interstitial He and the screw dislocation depends on the relative position of He to these strong binding sites.

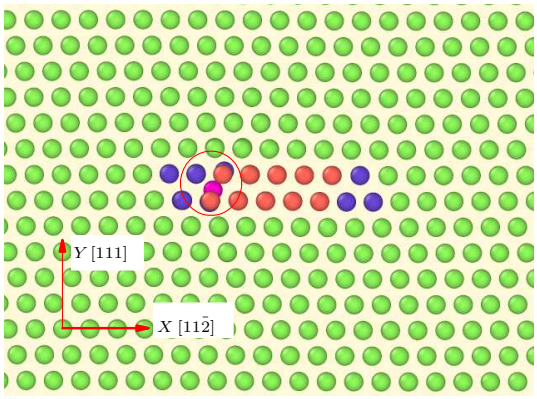

Fig. 4. The Crowdion configuration of [110] direction in the red circle area. The pink sphere is He and the green, blue, and red spheres represent fcc, non-fcc, and SF (i.e., hcp-structured) Ni atoms, respectively.

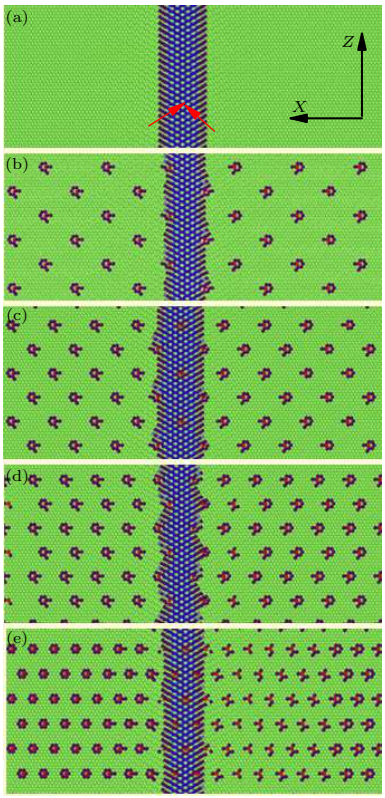

Fig. 5. Effects of He atoms uniformly distributed in the slip plane on screw dislocation dissociation: (a) dislocation configuration without He; (b) with 2.08% He; (c) with 3.36% He; (d) with 6.25% He; and (e) with 8.125% He. Ni atoms are colored according to the CNA and He atoms are indicated by red spheres. Here $\boldsymbol{b}$ are the burgers vectors denoted by the arrows.

Previous simulations have illustrated the marked influence of SFs on the mechanical behavior and microstructure of nanocrystals.[33,34] Hence, the effect of He on the SF width is an important aspect that influences both dislocation processes and mechanical properties. Here we use MD simulations to examine the effects of He atoms uniformly distributed in the slip plane on the dissociation of a screw dislocation in Ni.

The configuration of the screw dislocation after relaxation, as shown in Fig. 5(a), only Ni atoms below the slip plane are shown. The partial dislocations and SF region are outlined by purple and blue Ni atoms, respectively.

Helium atoms introduced in the slip plane affect the separation between partials, as shown in Figs. 5(b)–5(e). Figure 6 shows the dependence of the separation on the He content in the slip plane. The separation of partials decreases with He content up to 2.08%, and then increases reaching a maximum at 3.36%. With a further increase of the He content, the separation of partials decreases to 8.125%, above which no further effects of the He content are observed. The overall trend is that He atoms uniformly distributed in the glide plane initially reduce the separation between partials, which then remains constant above a certain He concentration. The decrease of SF width with increasing the He concentration can be explained as follows: according to the elastic theory, the stacking fault width $d_{\rm sf}$ is given by

$$d_{\rm sf} = \frac{\mu b^2}{24\pi\gamma_{\rm sf}} \frac{2+\nu}{1-\nu},$$

where μ is the shear modulus, ν is Poisson's ratio, $\gamma_{\rm sf}$ is the intrinsic stacking fault energy, and $b = \alpha_0/\sqrt{2}$ is the Burgers vector length of the full dislocation. Thus $d_{\rm sf}$ and $\gamma_{\rm sf}$ are inversely proportional whereas μ and ν only have minor effects at low He content. Hence, at low He content the decrease of separation is purely due to the increase of $\gamma_{\rm sf}$.

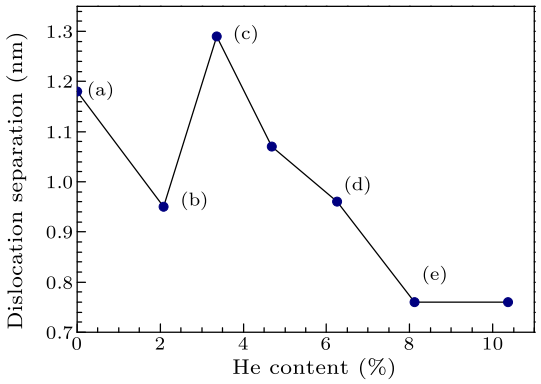

Fig. 6. Dependence of dissociation separation on He content.

In addition, the SF width in pure fcc metals was previously shown to depend mainly on the stable SFE.[35] The profile of the GSFE is an important measure of lattice resistance to shear.[36] To verify the above view, the GSFEs with and without He were calculated.

The GSFE profile for fcc Ni sheared by one period in the [11$\bar{2}$] direction along the (111) plane ($f = 3$) is shown in Fig. 7. This energy profile can reveal several important features of the slip, including the stable (or intrinsic) SFE $\gamma_{\rm sf}$ and the unstable SFE $\gamma_{\rm us}$. The former is typically associated with the width of the dissociated dislocation, and the latter defines the

energy barrier for the homogeneous nucleation of an SF. Further shear beyond point γ_{sf} ($f = 1$) on the GSFE curve along the $[11\bar{2}]$ direction results in another unstable structure at $f = 2$. Due to the local, high energy, unstable ...ABCAA... stacking, which corresponds to a global maximum SFE, denoted by γ_{max} here. It is noted that while both points $f = 0.6$ and $f = 2$ on the GSFE curve in Fig. 7 correspond to unstable structures, the respective fault energies, the required shear displacements and stacking sequences are completely different. It is therefore necessary to determine both γ_{us} and γ_{max} in addition to the intrinsic SFE for a complete description of the GSFE curve along the $[11\bar{2}]$ direction.

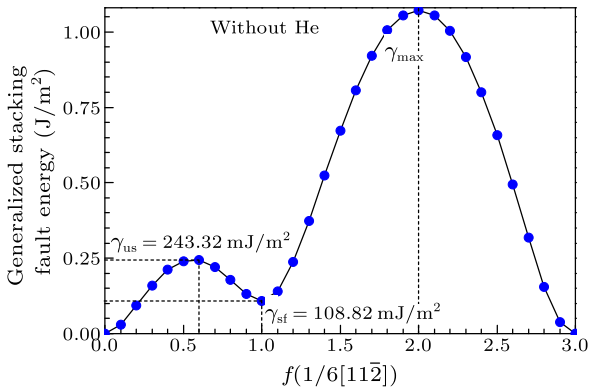

Fig. 7. Generalized stacking fault energy of the slip system without He on the glide plane.

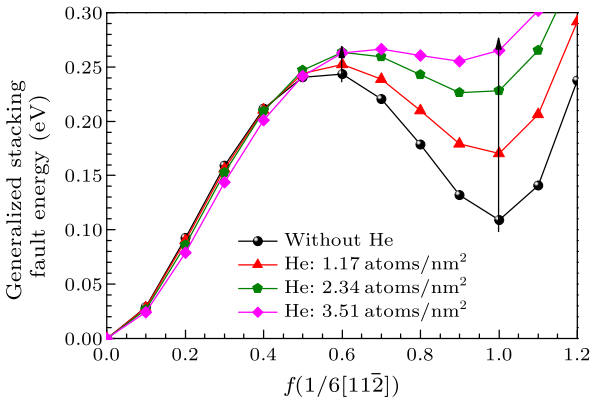

Fig. 8. Generalized stacking fault energy of the slip system with and without He on the glide plane.

From our simulations, γ_{sf} and γ_{us} are estimated to be $108.82\,mJ/m^2$ and $243.32\,mJ/m^2$, respectively, for perfect fcc Ni in the absence of He, which are in reasonable agreement with the experiments ($\gamma_{sf} = 125\,mJ/m^2$[25,37]). In the presence of He, the GSFE as a function of He concentration in the SF plane is shown in Fig. 8. The GSFE with He occupying the available T sites in the SF plane, giving an areal density of $1.17\,atoms/nm^2$, is shown as a red line in Fig. 8. The stable SFE clearly increases to $\gamma'_{sf} = 170.39\,mJ/m^2$, while the unstable SFE slightly increases to $\gamma'_{us} = 252.54\,mJ/m^2$, indicating a weaker impeding effect during shear. He concentrations of 2.34 and $3.51\,atoms/nm^2$ show a similar behavior, with the stable SFE clearly increasing with the He concentration. These observations thus explain the decreasing width of SF with increasing the He content.

The present results show that homogeneously distributed He atoms can decrease the separation between partials, and support the hypothesis that the increase of SFE caused by He induces slip planarity. The increasing SFE decreases the separation between partials, while the attraction causes the partials to move closer to each other.

In conclusion, atomistic simulations of effects of He on the dissociation of a screw dislocation in Ni have been conducted by using an embedded-atom method potential. The results clearly demonstrate that interstitial He at tetrahedral sites in the fcc structure region and near one of the two Shockley partial cores located on one plane above/below have the strongest binding energy. The interaction between interstitial He and the screw dislocation is clarified based on the relative position of He to these strongest binding sites. In addition, it is found that He atoms homogeneously distributed in the glide plane can decrease the SF width.

References

[1] Yvon P and Carré F 2009 *J. Nucl. Mater.* **385** 217
[2] Tancret F et al 2003 *Mater. Sci. Technol.* **19** 296
[3] Braski D N et al 1979 *J. Nucl. Mater.* **83** 265
[4] Ullmaier H 1984 *Nucl. Fusion* **24** 1039
[5] Wang H Y et al 2008 *Acta Phys. Sin.* **57** 3703
[6] Liang L et al 2015 *Acta Phys. Sin.* **64** 046103 (in Chinese)
[7] Rodney D 2004 *Acta Mater.* **52** 607
[8] Soleymani M et al 2014 *Comput. Mater. Sci.* **84** 83
[9] McReynolds A W et al 1955 *Phys. Rev.* **98** 418
[10] Rodney D and Martin G 1999 *Phys. Rev. Lett.* **82** 3272
[11] Xu Q, Yamasaki H et al 2011 *Philos. Mag. Lett.* **91** 724
[12] Xu Q, Yamasaki H et al 2013 *Mater. Sci. Eng.* A **586** 231
[13] Yang L et al 2010 *Physica* B **405** 1754
[14] Heinisch H L et al 2006 *J. Nucl. Mater.* **351** 141
[15] Plimpton S 1995 *J. Comput. Phys.* **117** 1
[16] Sheng H W et al 2011 *Phys. Rev.* B **83** 134118
[17] Aziz R A and Janzen A R 1995 *Phys. Rev. Lett.* **74** 1586
[18] Zhang W et al 2015 *J. Nucl. Mater.* (accepted)
[19] Brommer P and Gähler F 2007 *Modell. Simul. Mater. Sci. Eng.* **15** 295
[20] Ziegler J F et al 1985 *The Stopping and Range of Ions in Matter* (New York: Pergamon)
[21] Faken D and Jonsson H 1994 *Comput. Mater. Sci.* **2** 279
[22] Tsuzuki H et al 2007 *Comput. Phys. Commun.* **177** 518
[23] Stukowski A 2010 *Modell. Simul. Mater. Sci. Eng.* **18** 015012
[24] Cai W http://micro.stanford.edu/MDpp/
[25] Carter C B and Holmes S M 1977 *Philos. Mag.* **35** 1161
[26] Szelestey P et al 2003 *Modell. Simul. Mater. Sci. Eng.* **11** 883
[27] Xiang Y X and Yu W C 2013 *Chin. Phys.* B **22** 027101
[28] Wen M et al 2005 *Philos. Mag.* **85** 1917
[29] Angelo J et al 1995 *Modell. Simul. Mater. Sci. Eng.* **3** 289
[30] Rao S I et al 2010 *Acta Mater.* **58** 5547
[31] Hepburn D J et al 2013 *Phys. Rev.* B **88** 024115
[32] Zu X T et al 2009 *Phys. Rev.* B **80** 054104
[33] Aubry S and Hughes D A 2006 *Phys. Rev.* B **73** 224116
[34] Wolf D et al 2005 *Acta Mater.* **53** 1
[35] Hirth J P and Lothe J 1982 *Theory of Dislocations* (New York: Wiley)
[36] Vitek V 1968 *Philos. Mag.* **18** 773
[37] Zimmerman J A et al 2000 *Modell. Simul. Mater. Sci. Eng.* **8** 103